Selected Paper

Characterization of the Peroxidase Activity of Single Algae Protoplasts by Scanning Electrochemical Microscopy

Huafang Zhou, Shigenobu Kasai, Hiroyuki Noda, Hiroaki Ohya-Nishiguchi, Hitoshi Shiku,*,† and Tomokazu Matsue*,††,#,##

Institute for Life Support Technology, 2-2-1 Matsuei, Yamagata 990-2473

†Regional Joint Research Project of Yamagata Prefecture, Japan Science and Technology Corporation, 2-2-1 Matsuei, Yamagata 990-2473

††Department of Biomolecular Engineering, Graduate School of Engineering, Tohoku University, Aramaki Aoba, Sendai 980-8579

Received February 25, 2003; E-mail: matsue@bioinfo.che.tohoku.ac.jp

The peroxidase activity in a single protoplast of alga *Bryopsis plumosa* is quantitatively characterized by scanning electrochemical microscopy. The generation of ferriceniummethanol (FMA^+) at the protoplast surface is directly detected by the microelectrode tip scanned close to the sample surface in seawater containing ferrocenemethanol (FMA) and hydrogen peroxide, an electron mediator and an enzyme-substrate, respectively. The oxidation reaction requires hydrogen peroxide, which clearly shows FMA^+ generation due to the peroxidase (POD) catalytic reaction occurring in the protoplast. The FMA^+ generation and the FMA accumulation rates at a single alga protoplast were equivalent. A plot of the FMA^+ generation rates according to the hydrogen peroxide concentrations was well allowed with a Michaelis–Menten-type reaction. An estimation of the mass-transfer rate and a determination of the K_m are quite important advantages of the SECM technique that cannot be realized using other techniques. The POD activity has been further investigated from the viewpoint of the size of the protoplast. The POD activity of the alga in the adult stage is also visualized by SECM. The noninvasive nature of the SECM technique has been confirmed by observing the developmental process after measurements.

Scanning electrochemical microscopy[1–5] (SECM) has been widely applied in numerous fields, such as electrode surfaces, alloys, polymers, and biomaterials. Because of its technical advantage to characterize and image localized chemical reactions, it has been recognized as a powerful tool to probe the biochemical nature of various surfaces, including DNA,[6,7] enzymes,[8–12] antigen–antibody,[13–16] and lipids.[17–20] Pierce and Bard[9] characterized the enzymatic activity in individual mitochondrion fixed on a glass substrate. Yamada et al.[10] determined the Michaelis–Menten constant (K_m) of an immobilized enzyme at a glass substrate. Enzymes were used for labeling antigens or antibodies in studies for fabricating antibody-chips.[13–16] These reports mainly focus on a study of immobilized enzymes on a solid supports.

Amperometric and voltammetric methods utilizing a microeletctrode for probing single-cell functions have been played important roles for more than thirty years.[4] Extra-cellular detection schemes, as for studies using SECM or self-reference electrodes,[21] are advantageous to avoid both the injury to the living cells and contamination of the probe microelectrode surface. Neurotransmitters,[22–24] anti-cancer drugs,[25] and reactive oxygen species[26,27] have been directly detected with a microelectrode positioned very close to the single-cell surface. Photosynthetic and respiration activities have been quantitatively discussed.[28–37] Recently, the electron transfer[4,38–40] and permeation[41] of redox species at the single-cell level have been reported. However, to our knowledge, there has been no report concerning the detection of enzymatic activities of individual living cells. We firstly report here on an SECM study aimed at probing the enzymatic activity of a single cell, a living alga protoplast, under its physiological condition.

Experimental

Ferrocenemethanol (FMA, [Hydroxymethyl]ferrocene) was purchased from Aldrich Chem. Co. All chemicals were used as reagent grades. All aqueous solutions were prepared from distilled and deionized water by an AQUARIUS GS-200 (Advantec). Seawater was used after filtration and being treated in an autoclave at 110 °C for 20 min.

Protoplasts of the marine algae *Bryopsis plumosa* were prepared according to a method reported by Tatewaki and Nagata.[42] Briefly, a piece of algae was immersed into sea water, and the cytoplasma of the algae was squeezed out into the sea water using tweezers. The cytoplasma aggregated to form protoplasts after leaving for 10 to 30 min. The protoplast was cultivated in light irradiation (1.3 klx) at room temperature in seawater containing a 2% of growth medium. For the growth medium,[28] 175.5 mg $Fe(NH_4)_2(SO_4)_2 \cdot 6H_2O$, 175.5 mg H_3BO_3, 11.25 mg $FeCl_3 \cdot 6H_2O$, 41.0 mg $MnSO_4 \cdot 4H_2O$, 5.5 mg $ZnSO_4 \cdot 7H_2O$, 1.2 mg $CoSO_4 \cdot 7H_2O$, 415 mg Na_2EDTA, 5.0 mg thiamine hydrochloride, 0.1 mg vitamine B_{12}, 0.05 mg Biotin, 3.5 g $NaNO_3$,

Institute for Life Support Technology

Japan Science and Technology Corporation

Published on the web September 15, 2003; DOI 10.1246/bcsj.76.1757

0.5 g N_2glycerophosphate, and 5.0 g Tris buffer (Sigma) were prepared in 1.00 L of water.

A motor-driven XYZ-stage (Suruga Seiki, K701-20R) was located on the stage of an inverted microscope (Nikon TE300). Pt-microdisk electrodes sealed in a tapered soft-glass capillary (World Precision Instruments, PG10165-4) were fabricated according to the literature.[28,43] The tip potential was controlled with a potentiostat (Hokuto Denko, HA1010mM4). The oxidation current of FMA and the reduction current of FMA^+ were monitored at a tip potential of +0.5 and +0.1 V, respectively. The typical Pt-microdisk radius was 3.0 μm and the steady-state oxidation current was 400 pA in seawater containing 0.5 mM FMA. The radius of the tip, including the glass-sealed part, was less than 10 μm. The current profiles obtained by SECM measurements depend on the tip scanning rate and the scanning direction. In the case of a single line scanning at less than 2.4 μm/s with forward and back directions, the two current profiles still had apparent hysteresis. The SECM images were captured at a tip scanning rate of 14.7 μm/s, and showed only the profiles with the forward direction.

Analysis of the Mass-Transfer Rate Based on Spherical Diffusion Theory. The spherical diffusion theory has been widely used to quantify the mass-transfer rates at spherical sample surfaces in various SECM experimental systems.[4,38,44,45] The concentration profile according to the distance from the center of the spherical sample (L_O) is expressed as follows, when a sample with a spherical shape is placed in a solution under the conditions:

$$C = (C_s - C^*)r_s/L_O + C^*, \quad (1)$$

where the masstransfer rate by the sample is constant and the concentrations of the reactant and the product at the sample surface are uniform. Here, the r_s is the radius of the spherical sample, and C_s and C^* are the concentrations of the redox species at the sample surface and in the bulk, respectively. The distance from the center of the spherical sample is expressed as $L_O = r + r_s$, when the tip microelectrode is scanned according to the axis crossing the center of the sample. The r is the distance from the sample surface. The concentration difference between the bulk and the sample surface ($\Delta C = C^* - C_s$) is defined as the subtraction of the concentrations at $r_s/L_O = 0$ and 1. The flux density at the sample surface (f_s [mol cm^{-2} s^{-1}]) and the total masstransfer rate of the sample (F [mol s^{-1}]) are given by the following equations:

$$f_s = D\Delta C/r_s, \quad (2)$$

$$F = 4\pi r_s D\Delta C, \quad (3)$$

where D is the diffusion coefficient of the reagent. The D values of FMA and FMA^+ at room temperature are 7.0×10^{-6} cm^2 s^{-1}.[10] In the present study, the masstransfer rate of FMA^+ generation ($-F^{FMA^+}$) and FMA accumulation (F^{FMA}) are both expressed as the positive direction in the figures. For measuring ΔC, the tip was scanned back and forth at 14.7 μm/s for three times and the average ± standard deviation ($n = 6$) was estimated. The ΔC estimated by the scanning tip was identical within a 10% deviation to that obtained by the stationary tip at several points in a 500-μm scan range.[36]

In a previous study, we characterized the peroxidase (POD) activity of the tissue of a plant, celery (*Apium graveolens L.*).[46] The POD distribution at the cross section of the celery stem was visualized by an SECM measurement. A quantitative argument on the mass-transfer rate of the redox species was impossible because the POD molecules, themselves, come out from the cutting edge of the celery stem. In the case of alga protoplasts, however, the extraction of POD molecule from the sample surface seemed to be negligible, because it was confirmed that the membrane permeation of the protoplast[41] is very similar to that of the artificial bilayer lipid membrane.[17] The contribution of the direct release of the POD molecule to the F value estimated by the method mentioned above should be minor because the diffusion coefficient of the POD molecule is much smaller compared to that of the FMA and FMA^+.

Results and Discussion

An SECM image of POD activity in a single protoplast was obtained by two-dimensionally scanning the tip microelectrode to monitor the reduction current of FMA^+. Figure 1 shows an optical microscope photograph and an SECM image of a single protoplast with a radius of 81 μm in seawater containing 0.5 mM FMA and 0.5 mM H_2O_2. The SECM image was ob-

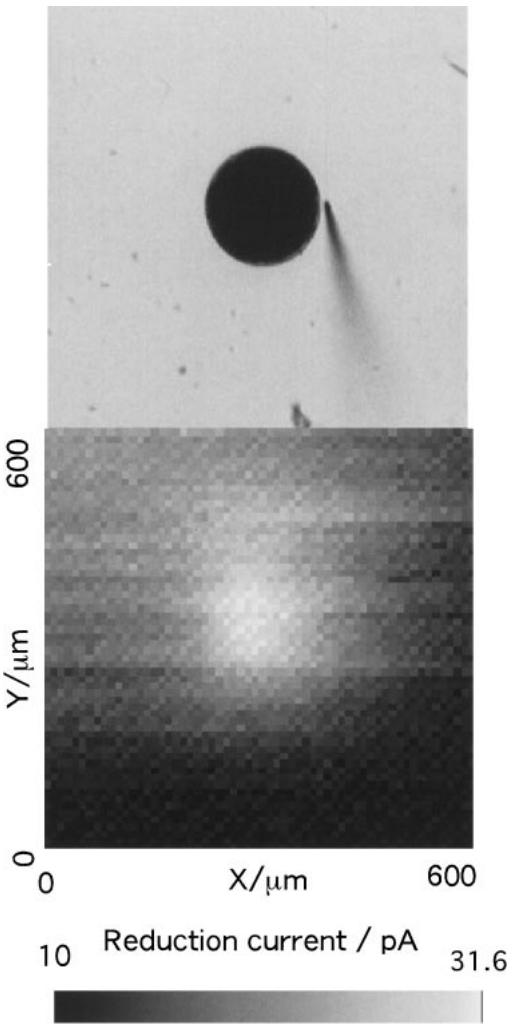

Fig. 1. An optical microscope photograph and an SECM image of the single protoplast with a radius of 81 μm in the seawater containing 0.5 mM FMA and 0.5 mM H_2O_2. The tip height from the top of the sample, 50 μm. The tip potential, +0.1 V vs Ag/AgCl. Tip radius, 3.0 μm.

tained at 50 μm height from the top of the sample surface. In the SECM image, the lighter region with the higher reduction current indicates that with the higher concentration of FMA^+ produced from the sample. Without H_2O_2 in the solution, the current increase near the single protoplast was not observed. Thus, The FMA is oxidized to FMA^+ in the presence of H_2O_2 by the POD catalytic reaction in the protoplast.

The FMA^+ production and FMA accumulation by the alga protoplast depend on the H_2O_2 concentration in the solution. Figure 2 shows the concentration profiles of FMA^+ and FMA near to a single protoplast with a 78 μm radius in solutions containing various concentrations of H_2O_2. In the experiments, the tip microelectrode was scanned according to the axis crossing the center of the sample. In the upper part of Fig. 2, the concentration profiles are shown as a function of the distance (r) from the sample surface. The profiles converted to C versus r_s/L_O plots as shown in the lower part of Fig. 2. A quantitative analysis on the POD activity of the protoplast is possible by using spherical diffusion theory. The lines in the figure are given by the method of least squares. The linearity of each plot is quite good. The concentration gradients increase for higher H_2O_2 concentrations, indicating that both FMA^+ production and FMA accumulation by the sample become larger for a higher H_2O_2 concentration. Again, the concentration profiles of both FMA^+ and FMA are totally flat without H_2O_2.

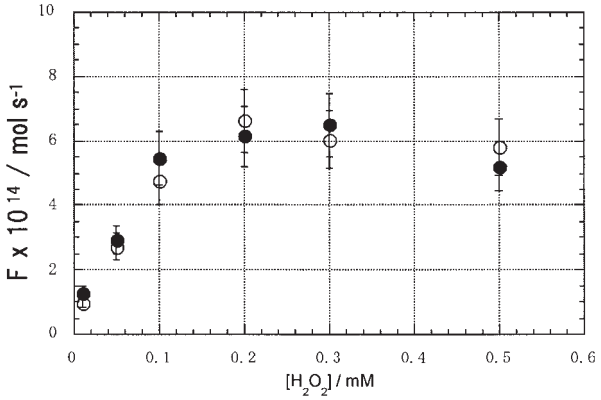

Fig. 3. The plot of the total fluxes (F) of the FMA^+ production (filled circles) and the FMA accumulation (open circles) by the single alga protoplast as a function of H_2O_2 concentration.

Figure 3 shows a plot of the total fluxes (F) of the FMA^+ production and the FMA accumulation by the single alga protoplast as a function of the H_2O_2 concentration. The filled and open circles indicate the F value of the FMA^+ production and the FMA accumulation, respectively. Basically, the FMA^+ production rate is comparable with the FMA accumulation rate, indicating that FMA is almost equivalently oxidized to FMA^+ by the POD-catalyzed reaction in the single cell.

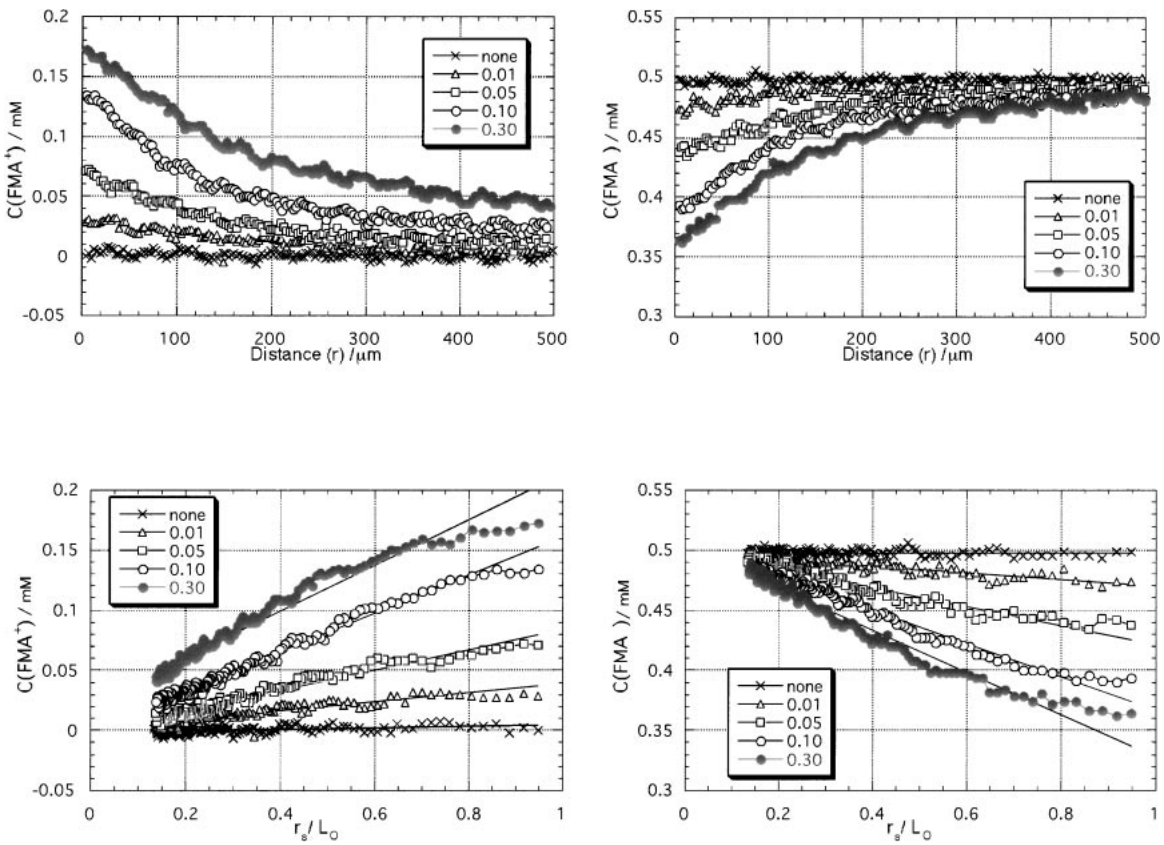

Fig. 2. (Upper) The concentration profiles of FMA^+ (C(FMA^+)) and FMA (C(FMA)) as a function of the distance (r) from the sample surface in the solution containing various concentrations of H_2O_2. The crosses, triangles, squares, open circles, and filled circles indicate the plots in 0, 0.01, 0.05, 0.10, and 0.30 mM H_2O_2 concentrations. The sample radius (r_s), 78 μm. (Lower) The C versus r_s/L_O plots.

One can see that the H_2O_2 concentration dependency of the flux is well explained by a Michaelis–Menten-type reaction. The fluxes linearly increase in the lower concentration region, and are saturated for higher concentration. The K_m for H_2O_2 was estimated as 53 ± 13 μM. It should be noticed that the K_m estimated here is an apparent value because several kinds of POD-isozymes (and other POD-like enzymes that catalytically oxidize FMA in the presence of H_2O_2) generally exist in living cells.[47–50] Although many methods have been used to characterize the POD activity of living cells and tissues,[47–49] the capacity of the SECM estimating the K_m value of the single living cell is noteworthy. The distribution of the K_m of the individual protoplast is also interesting. However, efforts to improve the measuring process should be required for comparing the K_m values of many protoplasts, because it takes 5 to 30 minutes until the concentration profiles of FMA^+/FMA reach a steady-state for each H_2O_2 concentration. The K_m value was smaller than 100 μM ($n = 2$), but, unfortunately we have no information whether K_m is a typical value for the alga *Bryopsis plumosa* at the present stage. Therefore, the POD activity was further characterized for many protoplasts in the condition of an excess amount of H_2O_2.

Figure 4 shows the POD activity as a function of the size (r_s) of the protoplast. The filled and open circles indicate the F value of the FMA^+ production and the FMA accumulation, respectively. The POD activity of the alga protoplast increases as the size of the protoplast becomes larger. In a previous study, we investigated the respiration and the photosynthesis activities as a function of the size of the protoplast.[37] We found that the respiration rate was linear to r_s^3; on the contrary, the photosynthesis rate was linear to r_s^2, suggesting that the former is controlled by the volume of the protoplast, and that the latter is controlled by the surface area of the protoplast. The results were explained by the geometrical distribution of the organelle, namely, mitochondrion homogeneously distribute in the cell; on the other hand, chloroplasts localize near the cell membrane. In the case of the POD activity, the slope of the log (F/mol s^{-1}) vs log (r_s/μm) plot was 2.4. This result indicates that the size-dependence of the POD activity of the alga protoplast is an intermediate situation between the respiration and the photosynthesis activities. Simultaneously, the result excludes the possibility that the permeation of the redox couple through the cell membrane of the protoplast is the rate-determining process, because the slope does not change for smaller and larger sizes of the protoplast.

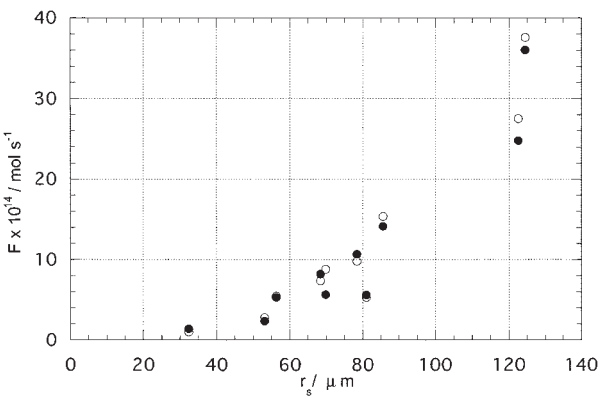

Fig. 4. The POD activity as a function of the size (r_s) of the protoplast. The filled and the open circles indicate the F of the FMA^+ production and the FMA accumulation, respectively. Measuring solution was the seawater containing 0.5 mM FMA and 0.5 mM H_2O_2.

Next, we demonstrated the SECM applicability for a noninvasive measurement. For a single alga protoplast with a 32-μm radius, shown in the top of Fig. 5, an SECM measurement was carried out to obtain the FMA^+ production rate as $1.03 \pm 0.073 \times 10^{-14}$ mol s^{-1}. After the SECM measurement in seawater containing 0.5 mM FMA and 0.5 mM H_2O_2, the protoplast was transferred into seawater containing a 2% growth medium. The photographs of the same protoplast one day and three days after the SECM measurement are shown in the middle and bottom of Fig. 5, respectively. This figure shows the noninvasiveness of the SECM in spite of the measurement performed in a solution containing an electron mediator (FMA) and an enzyme substrate (H_2O_2). The normal development and proliferation behaviors after the SECM measurements have already been reported.[36] In the present study, we have shown that the addition of an electron mediator or enzymatic substrate in the measuring solution is also possible to further cultivate living samples. Figure 6 shows an SECM image of the POD activity of an alga in the adult stage. The sample was destroyed with tweezers, as was done to prepare the protoplasts. The higher current region in the SECM image of the alga in the adult stage is well correlated with the region

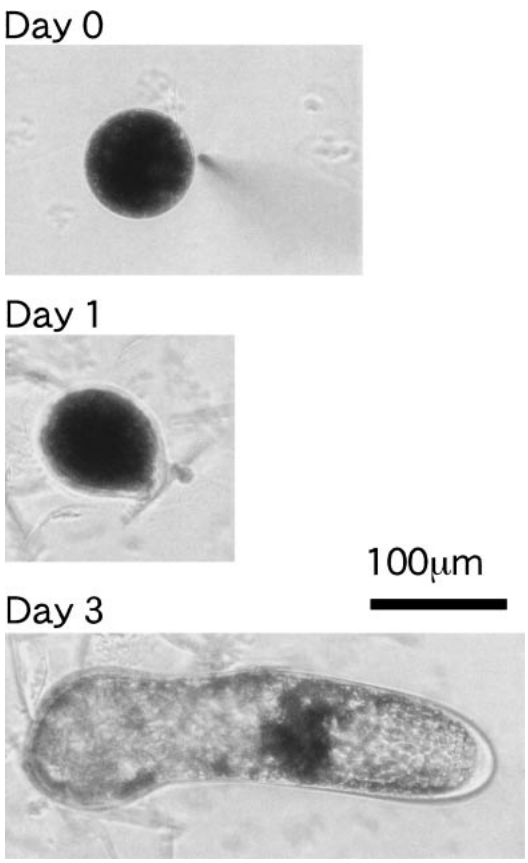

Fig. 5. Photographs of a protoplast at an SECM measurement (top), one day (middle) and three days (bottom) after the measurement.

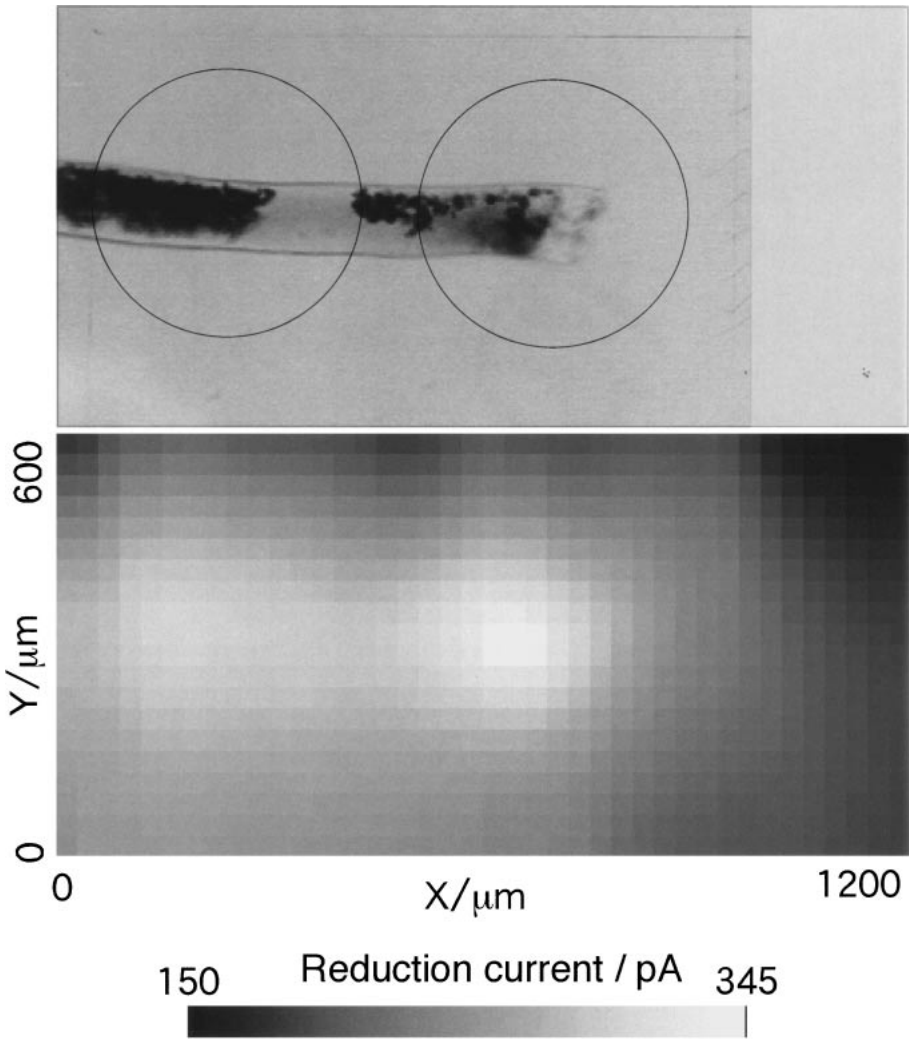

Fig. 6. A photograph and an SECM image of a piece of an alga in the seawater containing 0.5 mM FMA and 0.5 mM H_2O_2. The tip potential, +0.1 V vs Ag/AgCl. Tip radius, 7.0 μm. Measuring solution was the seawater containing 0.5 mM FMA and 0.5 mM H_2O_2.

existing in the cytoplasma surrounded by the cell wall. As is well known, the POD catalyzes various biochemical reactions in animal and plant cells to play important roles in the defense against physical and chemical stresses. Especially, the PODs of plants and bacteria function in the synthesis and repair of cell walls. The SECM technique will be useful to monitor among change of the POD activity in real-time.

The POD activity cannot be monitored in the case that samples contain an excess amount of reductant, such as ascorbic acid and polyphenols.[46] Besides, it is impossible to monitor the oxidation reaction catalyzed by POD when the electron mediators in the solution accept electrons from the electron-transfer chains existing in photosynthetic- or respiratory-metabolism. Yasukawa et al. reported that benzoquinone is reduced to hydroquinone in the alga protoplast both under dark and light-irradiation conditions.[4,38] We confirmed in the same single protoplast system that the reduction rate of FMA^+ is much smaller comparing to the oxidation rate of FMA catalyzed by POD. The light irradiation did not influence the FMA^+ production nor the FMA accumulation rate. Those results suggest that the oxidation/reduction behavior in the living sample largely depends on kinds of the living sample and the selected redox couple.[39–42,46] For example, FMA^+ production was not detected by approaching a probe microelectrode to a monolayer of mammalian cells (Chinese hamster ovary cell) on a culture dish in a phosphate buffer solution containing 0.5 mM FMA and 0.5 mM H_2O_2. This result points out the limitation of our method for monitoring the POD activity of mammalian cells. A further survey is required to select suitable redox species that efficiently permeate through the mammalian cell membrane in stead of FMA. For *chramidomonas reinhardtii*, which is a kind of unicellular green alga, the FMA^+ generation catalyzed by POD was detected in the same solution mentioned above when the *chramidomonas* exists on an agar-gel medium at the monolayer level.[51]

In conclusion, we first characterized an enzymatic activity at the single-cell level using the SECM technique in a solution containing an electron mediator and an enzymatic substrate. The POD activity of the individual protoplasts were further investigated as a function of the H_2O_2 concentration and the size of the protoplast. It may be possible to discuss the POD activity by comparing with the developmental potential or the other

metabolic activity of each single protoplast. The SECM technique will be useful in the future to monitor the change of the POD activity in real-time, in the developmental stage, response to wounding, and various conditions of cultivation.

This work was partly supported by Grant-in-Aid for Scientific Research (11227201) and a Grant-in-Aid for the Creation of Innovations through Business-Academic-Public Sector Cooperation (No. 13504) from the Ministry of Education, Culture, Sports, Science and Technology.

References

1 A. J. Bard, F.-R. F. Fan, J. Kwak, and O. Lev, *Anal. Chem.*, **61**, 132 (1989).
2 R. C. Engstrom and C. M. Pharr, *Anal. Chem.*, **61**, 1099A (1989).
3 "Scanning Electrochemical Microscopy," ed by A. J. Bard and M. V. Mirkin, Marcel Dekker Inc., New York (2001).
4 T. Yasukawa, T. Kaya, and T. Matsue, *Electroanalysis*, **12**, 653 (2000).
5 H. Shiku, H. Ohya, and T. Matsue, "Scanning Electrochemical Microscopy Applied to Biological Systems," in "Encyclopedia of Electrochemistry, Vol. 9, Bioelectrochemistry," ed by G. S. Wilson, Wiley-VCH (2002), Chapter 8, p. 257.
6 K. Yamashita, M. Takagi, K. Uchida, H. Kondo, and S. Takenaka, *Analyst*, **126**, 1210 (2001).
7 S. Takenaka, *Bull. Chem. Soc. Jpn.*, **74**, 217 (2001).
8 D. T. Pierce, P. R. Unwin, and A. J. Bard, *Anal. Chem.*, **64**, 1795 (1992).
9 D. T. Pierce and A. J. Bard, *Anal. Chem.*, **65**, 3598 (1993).
10 H. Yamada, H. Shiku, T. Matsue, and I. Uchida, *Bioelectrochem. Bioenerg.*, **33**, 91 (1994).
11 H. Zhou, S. Kasai, and T. Matsue, *Anal. Biochem.*, **290**, 83 (2001).
12 S. Kasai, Y. Hirano, N. Motochi, H. Shiku, M. Nishizawa, and T. Matsue, *Anal. Chim. Acta*, **458**, 263 (2002).
13 G. Wittstock, K. Yu, H. B. Halsall, T. H. Ridgway, and H. R. Heineman, *Anal. Chem.*, **67**, 3578 (1995).
14 H. Shiku, T. Matsue, and I. Uchida, *Anal. Chem.*, **68**, 1276 (1996).
15 C. A. Wijayawardhana, G. Wittstock, H. B. Halsall, and W. R. Heineman, *Anal. Chem.*, **72**, 333 (2000).
16 S. Kasai, A. Yokota, H. Zhou, M. Nishizawa, K. Niwa, T. Onouchi, and T. Matsue, *Anal. Chem.*, **72**, 5761 (2001).
17 H. Yamada, T. Matsue, and I. Uchida, *Biochem. Biophys. Res. Commun.*, **180**, 1330 (1991).
18 M. Tsionsky, A. J. Bard, and M. V. Mirkin, *J. Am. Chem. Soc.*, **119**, 10785 (1997).
19 M. Tsionski, J. Zhou, S. Amemiya, F.-R. F. Fan, A. J. Bard, and R. A. W. Dryfe, *Anal. Chem.*, **71**, 4300 (1999).
20 J. Zhang and P. R. Unwin, *J. Am. Chem. Soc.*, **124**, 2379 (2002).
21 S. C. Land, D. M. Poterfield, R. H. Sanger, and P. J. S. Smith, *J. Exp. Biol.*, **202**, 211 (1999).
22 D. J. Leszczyszyn, J. A. Jankowski, O. H. Vieros, E. J. Diliberto, Jr., J. A. Near, and R. M. Wightman, *J. Biol. Chem.*, **265**, 14736 (1990).
23 R. T. Kennedy, L. Huang, M. A. Atkinson, and P. Dush, *Anal. Chem.*, **65**, 1882 (1993).
24 T. K. Chen, G. Luo, and A. G. Ewing, *Anal. Chem.*, **66**, 3031 (1994).
25 H. Lu and M. Gratzl, *Anal. Chem.*, **71**, 2821 (1999).
26 S. Arbault, P. Pantano, I. A. Jankowski, M. Vuillaume, and C. Amatore, *Anal. Chem.*, **67**, 3382 (1995).
27 T. Yasukawa, A. Glidle, J. M. Cooper, and T. Matsue, *Anal. Chem.*, **74**, 5001 (2002).
28 S. Koike, Doctor Thesis, Graduate School of Engineering, Tohoku Univ. (1993).
29 M. Tsionsky, Z. G. Cardon, A. J. Bard, and R. B. Jackson, *Plant Physiol.*, **113**, 895 (1997).
30 T. Yasukawa, I. Uchida, and T. Matsue, *Denki Kagaku*, **66**, 660 (1998).
31 T. Yasukawa, Y. Kondo, I. Uchida, and T. Matsue, *Chem. Lett.*, **1998**, 767.
32 T. Yasukawa, T. Kaya, and T. Matsue, *Chem Lett.*, **1999**, 975.
33 T. Yasukawa, T. Kaya, and T. Matsue, *Anal. Chem.*, **71**, 4637 (1999).
34 S.-K. Jung, W. Gorski, C. A. Aspinwall, L. M. Kauri, and R. T. Kennedy, *Anal. Chem.*, **71**, 3642 (1999).
35 J. R. Trimarchi, L. Liu, D. M. Porterfield, P. J. S. Smith, and D. L. Keefe, *Biol. Reprod.*, **62**, 1866 (2000).
36 H. Shiku, T. Shiraishi, H. Ohya, T. Matsue, H. Abe, H. Hoshi, and M. Kobayashi, *Anal. Chem.*, **73**, 3751 (2001).
37 H. Shiku, T. Shiraishi, H. Ohya, T. Matsue, H. Abe, H. Hoshi, Y. Utsumi, S. Aoyagi, and M. Matsudaira, *Proc. Joint Symp. Bio-sens. Bio-imag.*, **2002**, 46.
38 T. Yasukawa, I. Uchida, and T. Matsue, *Biophys. J.*, **76**, 1129 (1999).
39 B. Liu, S. A. Rotenberg, and M. V. Mirkin, *Proc. Natl. Acad. Sci., U.S.A.*, **97**, 9855 (2000).
40 C. Cai, B. Liu, M. V. Mirkin, H. A. Frank, and J. F. Rusling, *Anal. Chem.*, **74**, 114 (2002).
41 T. Yasukawa, I. Uchida, and T. Matsue, *Biochim. Biophys. Acta*, **1369**, 152 (1998).
42 M. Tatewaki and K. Nagata, *J. Phycol.*, **6**, 40 (1970).
43 T. Matsue, S. Koike, and I. Uchida, *Biochem. Biophys. Res. Commun.*, **197**, 1283 (1993).
44 B. D. Bath, R. D. Lee, and H. S. White, *Anal. Chem.*, **70**, 1047 (1998).
45 B. R. Horrocks, M. V. Mirkin, D. T. Pierce, A. J. Bard, G. Nagy, and K. Toth, *Anal. Chem.*, **64**, 1795 (1992).
46 H. Zhou, H. Shiku, S. Kasai, H. Noda, T. Matsue, H. Ohya-Nishiguchi, and H. Kamada, *Bioelectrochemistry*, **54**, 151 (2001).
47 M. Hrubcova, M. Cvikrova, and J. Eder, *Biol. Plant.*, **36**, 175 (1994).
48 H. Narita, Y. Asaka, K. Ikura, S. Matsumoto, and R. Sasaki, *Eur. J. Biochem.*, **288**, 855 (1995).
49 J. D. Torkelson, J. A. Lynnes, and H. G. Werer, *J. Physiol.*, **31**, 562 (1995).
50 T. Gaspar, C. Penel, F. J. Castillo, and H. Greppin, *Physiol. Plant.*, **64**, 418 (1985).
51 H. Shiku, H. Uchida, Y. Hara, H. Ohya, H. Noda, and T. Matsue, Japanese Patent P2001-316387.